J Mol Model (2014) 20:2185
DOI 10.1007/s00894-014-2185-9

ORIGINAL PAPER

Roles of electrostatic interaction and dispersion in CH···CH, CH···π, and π···π ethylene dimers

Ye Cao · Ming Wah Wong

Received: 8 November 2013 / Accepted: 17 February 2014 / Published online: 28 March 2014

Abstract Ab initio molecular orbital calculations were performed up to the CCSD(T)/CBS level to investigate the roles of the electrostatic interaction and dispersion in three basic types of intermolecular interaction, namely CH···CH, CH···π, and π···π interactions, in D_{2d}, C_{2v}, and C_i ethylene dimers, respectively. SAPT energy decomposition revealed that the electrostatic interaction is more significant than expected, with its value being close to that of the net interaction energy. Dispersion is the largest stabilizing force and it plays the main role in balancing out exchange repulsion. This balance is related to the proposed concept of "contact." The roles of the σ and π electrons were distinguished in the electrostatic interaction by performing distributed multipole analysis and in dispersion by performing frozen-orbital SAPT (fo-SAPT) calculations. The electrostatic part of the interaction energy for each ethylene dimer can be understood as either a quadrupole–quadrupole attraction or the attraction between C and H atoms. (Electron pair)–(electron pair) contributions to the dispersion were calculated by the fo-SAPT method to shed light on the nature of dispersion. In these dimers, contributions to the dispersion can arise from π↔π, σ↔π, or σ↔σ electron-pair interactions. Surprisingly, σ↔π interactions dominate the dispersion in all three ethylene dimers. The π↔π contribution is very small, even in the displaced parallel structure (C_i). The σ↔σ interaction contributes to intermolecular binding by helping the dispersion to balance out exchange repulsion, but this interaction is limited to the most stable D_{2d} structure, which is characterized by four pairs of close dihydrogen contacts. The concept of an electron-pair "contact" was introduced to describe the exchange–dispersion balance. The D_{2d} dimer is stabilized by a large number of such contacts.

Keywords Ethylene dimer · Intermolecular interaction · Energy decomposition · π···π interaction · CH···π interaction

Introduction

Intermolecular interactions are vital in many aspects of chemistry and biology [1–3]. Without intermolecular interactions, no ordered or functioning materials—such as DNA—could form. The thermodynamic properties and kinetic characteristics of gases, liquids, and solids depend on the intermolecular potentials in which the molecules within the bulk move according to the thermal conditions. Transition states of elementary chemical reactions are also formed due to the interactions between reactants that collide [3]. There are different types of intermolecular interaction. When categorized by the nature of the interaction, there are (1) electrostatic interaction dominated interactions, such as hydrogen and halogen bonds [4], and attractive interactions between ions, (2) induction-dominated interactions, such as charge-transfer complexes, and (3) dispersion-dominated interactions, such as the attractions between noble gas atoms and π-stacking interactions between aromatic rings. Intermolecular interactions among π-electron-rich molecules are particularly interesting, because such molecules usually have large polarizabilities as well as high electron densities, meaning that they readily form dispersion-dominated complexes and attract positively charged atoms or molecules electrostatically [5–11]. A few types of interaction are associated with neutral π-electron-rich molecules. Among them, CH···π and π···π interactions are the most studied. CH···π interactions can be categorized as soft

Electronic supplementary material The online version of this article (doi:10.1007/s00894-014-2185-9) contains supplementary material, which is available to authorized users.

Y. Cao · M. W. Wong (✉)
Department of Chemistry, National University of Singapore,
3 Science Drive 3, Singapore 117543, Singapore
e-mail: chmwmw@nus.edu.sg

acid/soft base (SA/SB) interactions [12–14]. Dispersion usually dominates this type of interaction. In the case of activated CH···π interactions [15, 16], both electrostatic attraction and dispersion are important stabilizing forces. The strength and directionality of the CH···π interaction and the role of the electrostatic interaction are related to the acidity of the hydrogen donor. π-stacked structures were initially thought to be dominated by electrostatic interactions [17], since the preference for displaced parallel stacking over direct stacking could be understood by invoking quadrupole–quadrupole interactions. However, Podeszwa et al. later showed that the quadrupole–quadrupole interaction is not necessarily attractive for this configuration [6]. Studies of substituted complexes [18] and of SAPT components [6, 19, 20] have shown that dispersion is usually the largest contributor to the stabilization of these stacked structures.

Benzene is an archetypal π-electron-rich molecule with six π electrons that follows Hückel's $4n+2$ rule of aromaticity. Therefore, complexes of benzene are often used to study the interaction between the π-cloud and other molecules or ions. It is well established that the tilted T-shaped (perpendicular or edge-to-face) dimer (Scheme 1) is the most stable structure. However, the displaced parallel stacked structure (Scheme 1) has a similar stability to the CH···π structure [21]. In both forms of the dimer, the dominant attractive force is dispersion [5, 6, 22–24]. Studies of the fused rings have shown that the displaced parallel dimer becomes more stable than the T-shaped structure as the molecule increases in size [25, 26]. In addition, substitutions on the aryl rings stabilize the displaced parallel dimer more than the T-shaped dimer [27].

Surprisingly, ethylene—the simplest π-system, with only one pair of π electrons—is less well studied than benzene. A total of 14 possible structures of ethylene dimer have been examined via several molecular orbital calculations [28–31]. Other than the displaced parallel (C_i symmetry) and CH···π (C_{2v} symmetry) structures, another important geometry is a structure with four pairs of close dihydrogen contacts (D_{2d} symmetry) (Scheme 1). This is the most stable structure found for ethylene dimers. Several databases for weak interactions, such as S22 [32] and PPS5 [33], have included this structure as a prototypical system. There is evidence that the dihydrogen contacts in organic molecules contribute attractively to intermolecular interactions, due to the topological properties of the electron density [34] and the fact that the interaction energy increases with the number of dihydrogen contacts in dimers of *n*-alkanes [35, 36]. However, it is not clear whether these CH···CH contacts in the ethylene dimer are stabilizing or not. The nature of the intermolecular interaction was analyzed for various ethylene dimer configurations by different energy partition schemes [20, 29–31]. Dispersion and electrostatic interactions were identified as the major attractive forces that stabilize these dimers. The importance of the electrostatic interaction seems to have been overlooked.

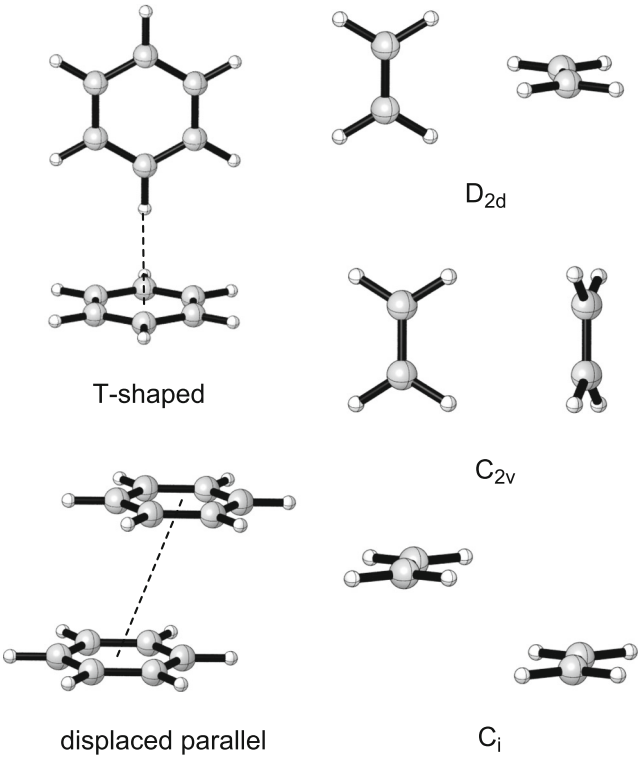

Scheme 1 Structures of benzene and methane dimers

Although the magnitude of the electrostatic stabilization is similar to that of the SAPT interaction energy, it is still considered less important than in some other complexes [20].

When studying the nature of the binding of complexes with π-electron-rich molecules, it would be useful to separate the contribution of π orbitals from that of the σ backbone, but such studies are rare. Based on a series of computations of aromatic compounds and their saturated counterparts, Grimme studied the role of π electrons in dispersion, and concluded that π···π stacking is missing in small π systems [37]. In this study, the contributions from π···π, σ···π, and σ···σ interactions to the MP2 correlation energy, instead of the dispersion energy, were separated. The electrostatic contribution was briefly discussed. The author examined only cyclic structures, not simpler linear molecules such as ethylene or butadiene.

Ethylene is the simplest system that has CH σ and π bonds. Therefore, the D_{2d}, C_i, and C_{2v} ethylene dimers are prototypical representations of CH···CH, π···π, and CH···π interactions, respectively. Due to its simplicity and symmetry, ethylene is a perfect model for separating σ and π contributions from the total electrostatic interaction and dispersion. The study reported in the present paper attempted to achieve such a separation for the three ethylene dimer configurations. The roles of σ and π electrons in the electrostatic interaction were investigated using distributed multipole analysis, and their roles in dispersion were analyzed by freezing some of the valence orbitals in the energy decomposition calculations.

This study also attempted to further characterize the nature of the CH···CH interaction and to understand the importance of the π···π interaction in this small π-system.

Computational methods

The structures of the three ethylene dimers (D_{2d}, C_i, and C_{2v}) and several related systems were optimized at the MP2/aug-cc-pVDZ level with and without counterpoise correction (CP and non-CP). Vibrational frequencies were calculated at the same level of theory to establish the nature of each stationary point. The interaction energies were evaluated using the CCSD(T) theory at the complete basis set (CBS) limit. The CCSD(T)/CBS energies were calculated as the sum of the MP2/CBS energies and a CCSD(T) correction term (CCSD(T)), evaluated with the aug-cc-pVDZ basis set. This additivity scheme takes advantage of the fact that the CCSD(T) and MP2 methods exhibit approximately the same basis set dependence [38]. The MP2/CBS energies were calculated using the extrapolation scheme of Halkier et al. [39], via directly computed aug-cc-pVDZ and aug-cc-pVTZ counterpoised energies. When extrapolation was used with the aug-cc-pVTZ and aug-cc-pVQZ basis sets, in combination with CCSD(T) single-point energy at the aug-cc-pVTZ level, the interaction energy improved by 0.01 kcal mol^{-1} for the three ethylene dimers. Thus, the smaller basis sets were used for the CBS extrapolation performed in this study. All geometry optimizations, frequency, and single-point energy calculations were performed using the Gaussian 03 suite of programs [40].

To analyze the nature of the stabilization of the ethylene dimers, we carried out symmetry-adapted perturbation theory (SAPT) [41] calculations up to the third order using the aug-cc-pVDZ basis set. This method allows for the separation of intermolecular interaction energies into well-defined components, namely the electrostatic interaction (ES), induction (IND), dispersion (DISP), induction–dispersion (IN-DI), and exchange repulsion (EX) terms. These terms are all calculated as the sum of selected energies in the SAPT analysis, and expressions for them are given in the "Electronic supplementary material" (ESM). Since the IN-DI term is very small in all systems (e.g., −0.05 kcal mol^{-1} for the ethylene D_{2d} dimer), it is not included in the tabulation. The total SAPT interaction energy (TOT) was calculated as the sum of various SAPT interaction components. For the larger complexes, such as substituted ethylene dimers and complexes involving benzene or butadiene, density functional theory–symmetry-adapted intermolecular perturbation theory (DFT-SAPT) [42–44] calculations with an aug-cc-pVDZ basis were performed instead of SAPT ones. The functional used was the PW91 correlation functional with 75 % PBE exchange mixed with 25 % HF exact exchange. To obtain the correct asymptotic behavior at long range, a shift was applied to the DFT-SAPT procedure [45]. The basis sets used for density fitting are the defaults employed in the MOLPRO program [46, 47]. The SAPT and density-fitting DFT-SAPT calculations were performed using the SAPT 2008 [48] and MOLPRO 2008 [46] programs, respectively.

It is important to note that the SAPT interaction energies calculated with the aug-cc-pVDZ basis set are known to be slightly underestimated with respect to (mainly) the dispersion energy [44]. Our own basis set benchmark calculations (Table 1) readily confirm this finding. The dispersion energy computed using aug-cc-pVDZ is underestimated by ~10 % compared to the triple-zeta estimate, while all other energy terms are relatively basis-set independent. Thus, a better estimate of the dispersion contribution can be obtained by scaling the aug-cc-pVDZ value. This scaling factor was chosen to be 15 % based on benchmark calculations for the methane dimer, ethyne dimer, and methane···N_2 complex [49]. It is also worth noting that the results obtained when using aug-cc-pVDZ result were better than those yielded by cc-pVTZ due to the importance of diffuse functions. As with previous benchmark studies on the DFT-SAPT method [44, 49], the total interaction energy of DFT-SAPT is more accurate than that of regular SAPT, while the dispersion energy is less favorable (Table 1). DFT-SAPT/aug-cc-pVDZ analysis of the ethylene D_{2d} dimer has been reported by Kim et al. [20]. Their calculated energy components are similar to our computed values, except for the induction term (Table 1). This difference is due to the fact that a different DFT functional was used and a different mathematical expression was employed for the induction term (see [20] and the ESM).

To gain insight into the individual (electron pair)–(electron pair) contributions to the dispersion, we decomposed the dispersion energy into contributions from orbital pairs. The contribution of the i^{th} and j^{th} orbitals in monomers A and B, respectively, is calculated in the following way:

$$E(i \leftrightarrow j) = E_{i-1,j-1} - E_{i,j-1} - E_{i-1,j} + E_{i,j},$$

where $E_{i,j}$ is the dispersion energy (calculated from Eq. 4 in the ESM) with orbitals 1–i on A, and 1–j on B frozen. This method, which we call frozen-orbital SAPT (fo-SAPT), ensures that the sum of contributions from all pairs equals the total dispersion energy, which is a desired property for a partition scheme. The SAPT program uses the "infinite excitation energy approximation" [50], so the separation of the exchange–dispersion term is a reliable approach. The third-order dispersion and exchange–dispersion terms are more complicated than the second-order terms because they include double sums and even triple sums of the contributions of the occupied orbitals of each monomer. A double sum implies that there is no unique way to separate the contribution of each orbital. Since the frozen-orbital approach decomposes the

Table 1 Comparison of the SAPT interaction energy contributions of the ethylene D_{2d} dimer (in kcal mol^{-1}) using correlation-consistent basis sets[a]. Calculated CCSD(T)/CBS interaction energy is −1.50 kcal mol^{-1}

SAPT term[b]	SAPT AVDZ	SAPT VTZ	DFT-SAPT AVDZ	DFT-SAPT VTZ	DFT-SAPT AVTZ	DFT-SAPT AVDZ[e]
ES	−1.21	−1.22	−1.25	−1.28	−1.25	−1.18
EX	2.64	2.52	2.65	2.65	2.65	2.68
IND	−0.09	−0.08	−0.08	−0.08	−0.09	−0.23
DISP[c]	−2.43 (−2.79)	−2.23 (−2.57)	−2.38 (−2.74)	−2.24 (−2.35)	−2.64 (−2.77)	−2.56
TOT[d]	−1.14 (−1.50)	−1.07 (−1.41)	−1.23 (−1.59)	−1.11 (−1.22)	−1.50 (−1.63)	−1.29

[a] AVDZ, ATZ, and AVTZ refer to aug-cc-pVDZ, cc-pVTZ, and aug-cc-pVTZ, respectively

[b] SAPT analysis up to the third order was conducted, while only second-order DFT-SAPT components were used. The induction–dispersion term (IN-DI) is around −0.05 kcal mol^{-1}, which is not shown in this table but included in the total SAPT interaction energy

[c] The numbers in parentheses are dispersion interaction energies scaled up by 15 % and 4 %, respectively, for double and triple zeta basis sets, as suggested in [49]

[d] The total interaction energy in SAPT does not include the δE_{HF} term, since third-order induction is explicitly considered, but the total interaction energy for DFT-SAPT does. Scaled dispersion is used to calculate the total interaction energies in parentheses

[e] From [20]

orbital contributions in only one of the many ways possible, it may not be considered rigorous. Nevertheless, this approach does at least provide energy components that sum to the total dispersion energy. We consider our proposed approach an acceptable method for obtaining good qualitative results. It is important to note that the third-order dispersion and dispersion–exchange terms constitute only a very small portion of the total dispersion energy. The effect of these terms on the orbital-pair analysis is shown in Table S2 of the ESM. Essentially, our proposed fo-SAPT approach provides an estimate of the contribution of a particular (electron pair)–(electron pair) interaction between two monomers (e.g., σ−σ, σ−π, or π−π), towards the total dispersion energy. We will employ the symbol "↔" to denote this type of (electron pair)–(electron pair) interaction, e.g., σ↔π, throughout the text.

Topological analysis was performed with the MORPHY98 program [51] based on MP2/aug-cc-pVDZ densities. Distributed multipole analysis was performed with the GDMA program [52], and electrostatic interaction energies between the multipoles were calculated using the ORIENT program [53].

Results and discussion

Structures and interaction energies of ethylene dimers

In the study reported here, we focused on just three ethylene dimeric forms, namely the D_{2d}, C_i, and C_{2v} dimers. The optimized geometries are given in Fig. 1. The D_{2d} structure has four sets of intriguing close dihydrogen contacts (2.55 Å). The best calculations reported for this D_{2d} dimer include the W1 method [33] and the CCSD(T) calculation with the quadruple zeta basis set [32]. The optimized geometry obtained at the MP2/aug-cc-pVDZ level (Fig. 1) is very close to the best geometries reported in the literature (see Table S1 in the ESM). The calculated CCSD(T)/CBS interaction energy is −1.50 kcal mol^{-1}, (−1.51 kcal mol^{-1} if two-point extrapolation with the aug-cc-pVTZ or aug-cc-pVQZ basis is used), in excellent agreement with the database value of −1.51 kcal mol^{-1} [32].

The stacked form of ethylene dimer is the simplest π-stacking structure. The ethylene sandwich dimer, with D_{2h} symmetry, has been studied. However, it is not a bound structure because of the repulsive quadrupole interactions present [54–56]. Similar to the benzene dimer, displaced parallel ethylene dimer configurations are structures of considerable interest. Two such ethylene dimeric structures have been examined by Suzuki et al. [28]. One has a similar nature to the sandwich dimer, while the other possesses attractive electrostatic interaction energy, and is the structure (C_i symmetry) investigated in this study. At the MP2/aug-cc-pVDZ level, with and without counterpoise correction, the optimized C_i structure has one imaginary frequency. A thorough scan of the potential energy surface (PES) of this ethylene dimer was conducted. In our PES scan, the molecular planes of both

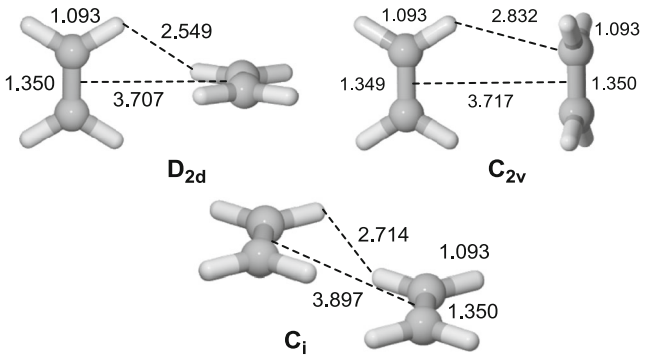

Fig. 1 Optimized (MP2/aug-cc-pVDZ, non-CP) geometries of the D_{2d}, C_{2v}, and C_i ethylene dimers. Bond distances are in Å

ethylene molecules were kept parallel and the C=C and C–H bonds were fixed. The center of one molecule was fixed at the origin and the C=C bond was considered the *z*-axis. Hence, the position of the other ethylene molecule can be described by the three parameters r, θ, and ϕ in a spherical coordinate system (Fig. 2).

The best optimized C_i structure calculated at the CCSD(T)/CBS level has r=4.0 Å, θ=30°, and ϕ=70°, and an interaction energy of −1.13 kcal mol^{-1}. It is worth noting that the extrapolated interaction energy for this geometry when using the aug-cc-pVTZ and aug-cc-pVQZ basis sets is also −1.13 kcal mol^{-1}. In this best π-stacking structure, the intermolecular C···H distance, i.e., r(C···H), is 3.2 Å, and the distance between the center of one molecule and the nearest H atom in the other is also 3.2 Å. This suggests the possibility of a CH···π interaction in the C_i dimer.

The second most stable form of ethylene dimer is the C_{2v} structure, which is characterized by two CH···π interactions. This C_{2v} dimer has a slightly smaller interaction energy than the D_{2d} dimer, despite the similar intermolecular distances of the two dimers. The optimized geometry of the C_{2v} dimer calculated at the MP2/aug-cc-pVDZ level is also shown in Fig. 1. The changes observed in the C=C and C–H bond lengths upon transitioning from the monomer to the dimer are very small, less than 0.0001 Å. The intermolecular C···H distance (2.83 Å) is characteristic of typical/nonactivated CH···π interactions [8, 13, 57–60], The calculated CCSD(T)/CBS interaction energy of this C_{2v} dimer is −1.08 kcal mol^{-1} (−1.09 kcal mol^{-1} with the larger basis), which is very close to that of the displaced parallel dimer (−1.13 kcal mol^{-1}).

Symmetry-adapted perturbation theory

The SAPT energy contributions of the three ethylene dimers are listed in Table 2, together with some related complexes. A plot of various SAPT components of the D_{2d} complex against intermolecular distance is shown in Fig. 3. The induction and induction–dispersion terms are always small; this is similar to what is seen for the benzene dimer [5, 24]. At all distances, all of the SAPT components are attractive except for exchange repulsion. Dispersion is the main source of stabilization; its magnitude is comparable to that of exchange repulsion. Due to their different decay rates, exchange repulsion is greater than dispersion when the intermolecular distance is less than the equilibrium distance, while dispersion is greater than exchange repulsion when the intermolecular distance is more than the equilibrium distance.

To provide further insight into why the D_{2d} dimer is the most stable ethylene dimer, it is essential to determine the kinds of interactions that are present in the dimer. To this end, we calculated the (electron pair)–(electron pair) contributions to dispersion using the fo-SAPT method. For the D_{2d} dimer, the

Table 2 SAPT interaction energy contributions (in kcal mol^{-1}) for various ethylene dimers and related dimers

Species	ES	EX	IND	DISP[e]	TOT	CBS[f]
$(C_2H_4)_2$ D_{2d} [a]	−1.21	2.64	−0.09	−2.79	−1.50	−1.50
$(C_2H_4)_2$ C_i [a]	−1.04	2.07	−0.07	−2.07	−1.15	−1.13
$(C_2H_4)_2$ C_{2v} [a]	−1.22	2.96	−0.09	−2.65	−1.05	−1.08
$(C_2H_4)_2$ D_{2d} [b]	−1.25	2.65	−0.08	−2.74	−1.59	−1.50
$(C_2H_4)_2$ C_i [d]	−1.05	2.05	−0.06	−2.02	−1.26	−1.13
$(C_2H_4)_2$ C_{2v} [b]	−1.18	2.89	−0.09	−2.58	−1.30	−1.08
(CH_4–benzene) [b,c]	−1.55	4.32	−0.16	−3.82	−1.50	
(C_2H_2–benzene) [b,d]	−2.91	5.55	−0.55	−4.32	−2.95	

[a] SAPT/aug-cc-pVDZ calculation

[b] DFT-SAPT/aug-cc-pVDZ calculation

[c] Similar calculations are also available in [59]

[d] Similar calculations are also available in [8]

[e] Dispersion is scaled up by 15 %

[f] CCSD(T)/CBS value

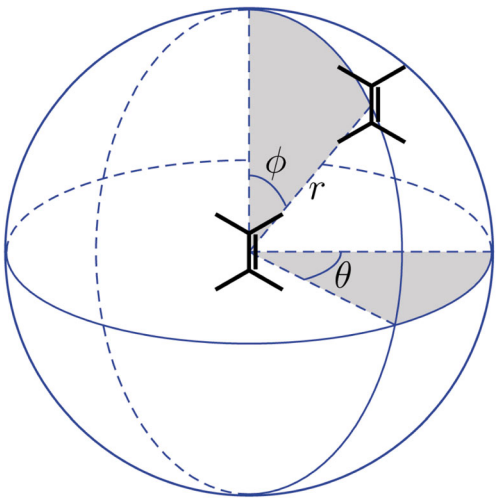

Fig. 2 Coordinate setup for the potential energy scan of the C_i ethylene dimer

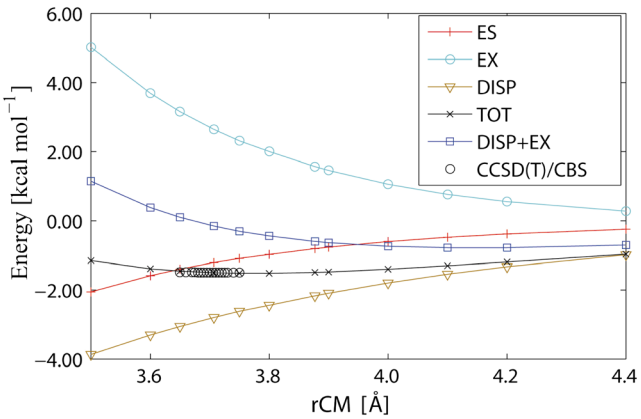

Fig. 3 Distance (rCM) dependence of SAPT components of the D_{2d} ethylene dimer. Dispersion energy is scaled up by 15 %

results (Table 3) indicate that the electron pairs that contribute the most to dispersion are the CC π-electron and two CH σ-electron pairs. Three types of (electron pair)–(electron pair) interactions are possible: π↔π, σ↔π, and σ↔ σ interactions. A π↔π interaction does occur in the D_{2d} dimer, but it is not as strong as the σ↔π and σ↔σ interactions. Close contact between two positively charged hydrogen atoms during interactions between C–H bonding electrons, e.g., #3↔#5 (Table 3), contributes significantly to attractive dispersion. This contribution is almost as large as that of the σ↔π interaction.

The optimum structural parameters for the C_i dimer at CCSD(T)/CBS level are rCM=4.0 Å and r(C···H) =3.2 Å, which are longer than those in the D_{2d} dimer (rCM=3.7 Å and r(C···H) =3.1 Å). Therefore, all ofthe SAPT components in the C_i dimer are smaller than their corresponding terms in the D_{2d} dimer (Table 2). Comparing the (electron pair)–(electron pair) contributions to the dispersion for the C_i (Table 3) and D_{2d} structures, we observe that the C_i dimer makes a smaller contribution to the dispersion because the σ↔σ interaction is missing. A scanned SAPT decomposition with rCM kept at 4.25 Å (Fig. 4) reveals how the attractive and repulsive terms compensate for each other, resulting in a displaced parallel structure.

As demonstrated by Fig. 4a, the electrostatic interaction is repulsive if the two ethylene molecules are directly on top of each other (i.e., $\theta=\phi=90°$); it becomes attractive when one molecule approaches the edge of the other molecule, similar to

Table 3 (Electron pair)–(electron pair) contributions to the dispersion (in kcal mol^{-1}) for the D_{2d}, C_i, and C_{2v} ethylene dimers[a]

D_{2d}	#1	#2	#3	#4	#5	#6
#1	−0.01	−0.01	−0.04	−0.01	−0.03	−0.03
#2	−0.01	−0.02	−0.05	−0.02	−0.05	−0.06
#3	−0.04	−0.05	−0.17	−0.05	−0.15	−0.15
#4	−0.01	−0.02	−0.05	−0.02	−0.05	−0.07
#5	−0.03	−0.05	−0.15	−0.05	−0.13	−0.20
#6	−0.03	−0.06	−0.15	−0.07	−0.20	−0.16
C_i	#1	#2	#3	#4	#5	#6
#1	0.00	−0.01	−0.02	−0.01	−0.02	−0.03
#2	−0.01	−0.01	−0.03	−0.01	−0.03	−0.06
#3	−0.02	−0.03	−0.06	−0.03	−0.07	−0.14
#4	−0.01	−0.01	−0.03	−0.02	−0.04	−0.07
#5	−0.02	−0.03	−0.07	−0.04	−0.08	−0.18
#6	−0.03	−0.06	−0.14	−0.07	−0.18	−0.16
C_{2v}	#1	#2	#3	#4	#5	#6
#1	−0.01	−0.01	−0.03	−0.01	−0.03	−0.02
#2	−0.01	−0.02	−0.04	−0.02	−0.06	−0.03
#3	−0.01	−0.02	−0.04	−0.02	−0.05	−0.05
#4	−0.01	−0.02	−0.03	−0.02	−0.05	−0.03
#5	−0.01	−0.02	−0.05	−0.03	−0.07	−0.06
#6	−0.07	−0.13	−0.36	−0.14	−0.43	−0.28

[a] #1 to #6 are valence electron pairs of ethylene. #3 and #5 are the CH σ-electron pairs, and #6 is the CC π-electron pair (see Fig. S2 in the ESM)

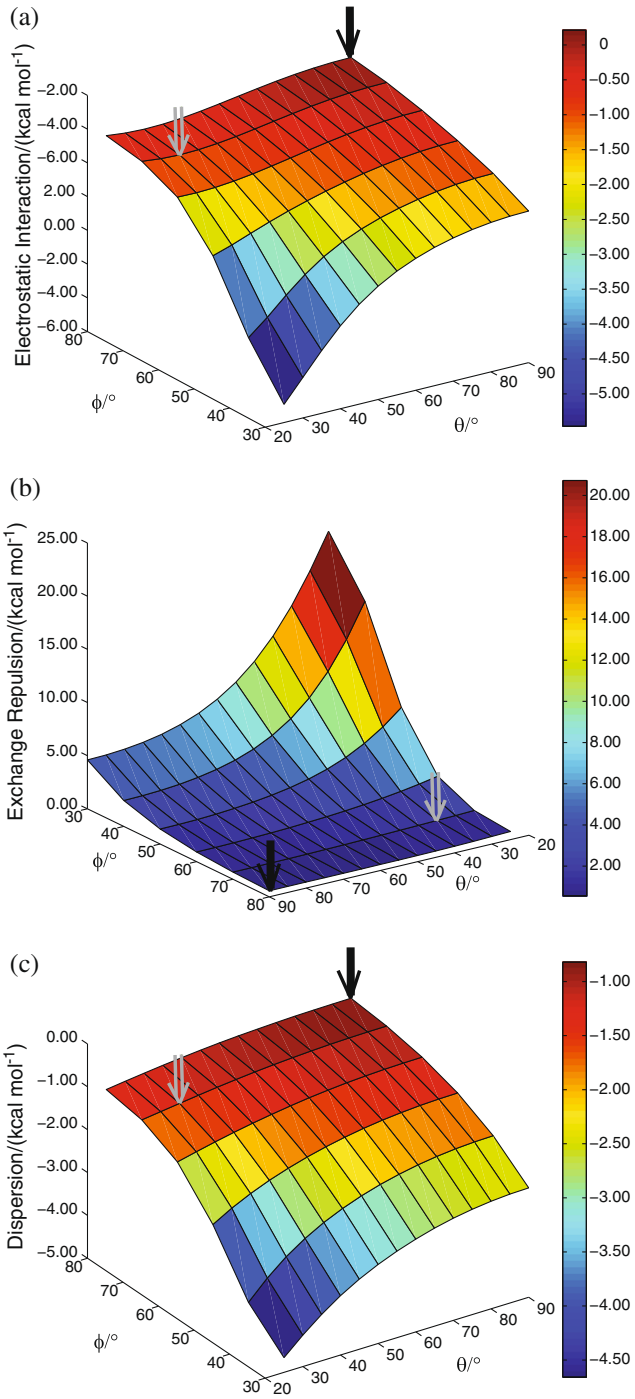

Fig. 4 Plots of SAPT components for the C_i ethylene dimer at rCM= 3.7 Å: **a** electrostatic interaction, **b** exchange repulsion, and **c** dispersion. The *hollow arrow* indicates the lowest energy minimum and the *solid arrow* shows the face-to-face stack structure

what is seen for the benzene dimer [17]. The electrostatic effect will be discussed in the next section.

Interestingly, the dispersion follows the same trend as the electrostatic interaction (Fig. 4c). Minimal dispersion occurs at $\theta=\phi=90°$. Direct stacking should favor π↔π interactions. Indeed, the contribution of π↔π to the dispersion in the direct

stacking geometry ($\theta=\phi=90°$) is −0.46 kcal mol^{-1}. At the optimum π-stacking geometry, the contribution of π↔π to the dispersion is only −0.16 kcal mol^{-1}, which is significantly smaller than that in the direct stacking structure. Despite the favorable π↔π interaction in the direct stacking geometry, the dispersion is minimal for this geometry and increases as θ and ϕ decrease. When θ and ϕ are small, the σ↔π contribution is greater than the π↔π contribution because there is a better chance that the H and π electrons will be in close contact. The (electron pair)–(electron pair) contribution to the dispersion in the CCSD(T)/CBS optimized geometry support this view. The interaction between the CH bonding σ-electron pair and the π-electron pair is much larger than that between the two π-electron pairs (Table 3).

Both the electrostatic interaction and the dispersion favor smaller θ and ϕ values. However, at small θ and ϕ, the electron density overlaps greatly, which leads to very large exchange repulsion. This is how the displaced parallel structure comes about. The attractive electrostatic and dispersion interactions share the same trend, and together they offset the repulsive exchange, achieving the optimum structure for quadrupole interactions and σ↔π interactions.

The C_{2v} ethylene dimer (Fig. 1) is considered the best configuration for quadrupole interactions [56]. This is readily reflected in the relatively large attractive electrostatic interaction term among the ethylene dimers. The proportions of dispersion and electrostatic interactions in the total SAPT interaction energy of the C_{2v} ethylene dimer is similar to that of the benzene–methane complex (Table 2), so it is best considered a nonactivated CH···π system [15, 16]. The C_{2v} ethylene dimer has similar electrostatic and dispersion components to the D_{2d} dimer, but it has a smaller interaction energy due to the larger exchange repulsion (Table 2).

The (electron pair)–(electron pair) contributions (Table 3) show more details in the intermolecular interaction for the C_{2v} dimer. The major contribution to the dispersion comes from the interaction between the π-electron pair from the H acceptor molecule and four (out of five) C–H σ-electron pairs of the H donor. Although the total number of significant interactions between electron pairs is smaller than in the D_{2d} dimer, each interaction term has a larger stabilizing energy. As a result, the total contribution to dispersion is comparable to that of the D_{2d} dimer. A smaller contribution to the dispersion comes from the interaction between the π-electron pairs, although this contribution is significantly larger than those in the C_i and D_{2d} dimers (Table 3). This means that π↔π interactions are not restricted to the stacked geometry. Indeed, a π↔π contribution to the dispersion is common to all three ethylene dimers.

The plot of SAPT components versus intermolecular distance (Fig. 5a) is very similar to that seen for the D_{2d} dimer, except that the point at which the dispersion attraction and exchange repulsion cancel each other out occurs at a larger distance. The fact that σ↔σ interactions and some σ↔π

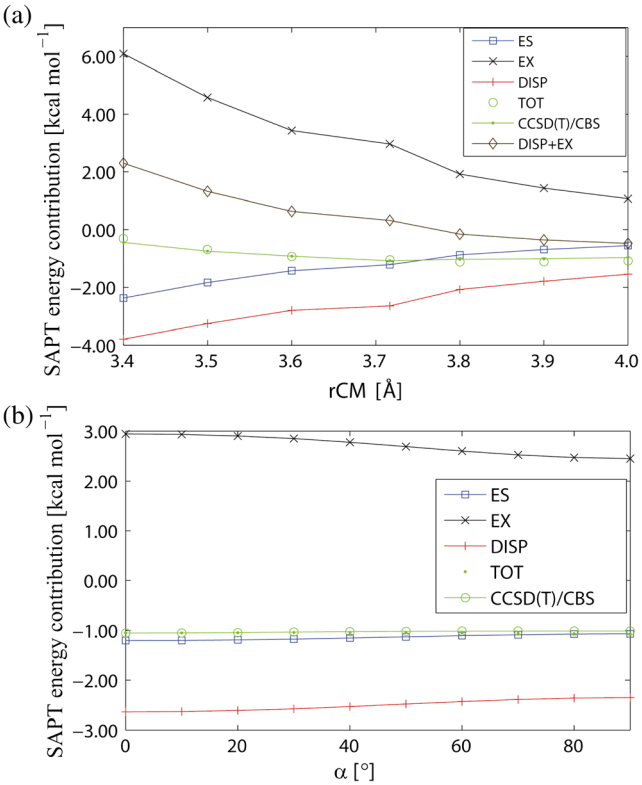

Fig. 5 Plots of SAPT components of the C_{2v} ethylene dimer with respect to **a** intermolecular distance (rCM) and **b** H-donor rotation angle (α). All dispersion energies are scaled up by 15 %

interactions are missing from the C_{2v} dimer may suggest that more (electron pair)–(electron pair) interactions in dispersion help to cancel out the exchange repulsion. Next, we compared the D_{2d} and C_{2v} structures by connecting them through a rotated CH···π structure. If we define α to be the H-donor rotation angle, a rotation of $\alpha=90°$ does not change the total interaction energy significantly (Fig. 5b). This is achieved through the canceling effect of decreasing the electrostatic interaction, dispersion, and exchange repulsion. When this rotated CH···π dimer is compared to the D_{2d} dimer, most structural parameters—such as the intermolecular distance between the centers of mass, the distance between the H atom and the center of the other ethylene molecule—stay almost the same. The most significant difference is in the H···H distance; the rotated CH···π structure has a distance of 3.06 Å while the D_{2d} structure has a shorter distance of 2.55 Å. Three (electron pair)–(electron pair) interaction terms contribute significantly to the dispersion in the rotated CH···π dimer, compared to nine in the D_{2d} dimer. The total contribution to the dispersion in the D_{2d} dimer is 0.39 kcal mol^{-1} larger than that in the rotated CH···π dimer, while the exchange is only larger by 0.19 kcal mol^{-1}. Both the number of significant (electron pair)–(electron pair) interactions and the changes in exchange repulsion and dispersion indicate that the σ↔σ interaction does aid dispersion in the dispersion–exchange balance, leading to more intermolecular binding.

The number of significant (electron pair)–(electron pair) interactions in dispersion is determined by the number of electron pairs that are in "contact" between the two monomers, and definitely affects the balance between dispersion and exchange. Here, we introduce the term "contact" as the number of significant (electron pair)–(electron pair) interactions, whereas "significant" is defined to be larger than twice the standard deviation of all the electron-pair interactions in dispersion. In the case of ethylene dimer, the magnitude of the ratio of exchange compared to dispersion decreases as the "contact" increases.

Table 4 summarizes the number of contacts in each of the three ethylene dimer configurations. If the number of contacts is large, the increase in exchange repulsion due to the short intermolecular distance will be compensated for by the dispersion interactions between more electron pairs. As a result, the two molecules in the complex are allowed to get closer to each other. For the ethylene dimers, the electrostatic interaction becomes more negative when the intermolecular distance shortens, leading to an increase in the total interaction energy. This argument readily explains the role of σ↔σ interactions in the intermolecular binding. The existence of an σ↔σ interaction results in a wider interaction area, allowing the monomers to approach each other more closely, which enhances the electrostatic attraction in the C···H interaction. Similar analyses (Table 5) performed for other related dimers, namely ethane and butadiene dimers, confirm that increasing the contact reduces the exchange/dispersion ratio. This lends further support to our argument.

The concept of contact has been used for alkane dimers in order to understand their stability [36], but this concept is mainly related to structural parameters rather than electron-pair interactions. One disadvantage of such a structure-based definition is that it is difficult to count the number of contacts because there is no well-defined cutoff distance that indicates whether a pair of atoms/groups are in contact. Although it may require tedious calculations, our electron-pair-based definition will usually give a definite value for the number of contacts, which can then be used to understand the stabilities of complexes.

Charge density analysis

The presence of an σ↔σ interaction in the D_{2d} ethylene dimer is also supported by electron density topology analysis, based on Bader's theory of atoms in molecules (AIM) [61, 62]. For each pair of H atoms in close contact, there is a bond path linking the two hydrogen atoms (Fig. 6b). Hence, there are four bond critical points in total (Fig. 6a). The positive sign of $\nabla^2\rho$ indicates that the interaction is closed shell in nature, e.g., a hydrogen bond [61, 62]. The small ρ and positive $\nabla^2\rho$ values (Table 6) are similar to the characteristic topological properties of a weak hydrogen bond, such as CH···O [63, 64] and CH···π [58, 65] interactions. An alternate geometry of the D_{2d} dimer in which the CH_2 terminal ends of the ethylene molecules face each other does not show any significant σ↔σ interaction. Accordingly, no bond critical point is found between the hydrogen atoms.

As expected, the C_{2v} ethylene dimer is characterized by two bond critical points (Fig. 6a). Each bond path links one hydrogen atom with one carbon atom of another ethylene molecule (Fig. 6b). The small ρ and positive $\nabla^2\rho$ values (Table 6) are comparable to those found in typical CH···π interactions [58, 65]. For the C_i dimer, one bond critical point is found (Fig. 6a). The ρ and $\nabla^2\rho$ values are fairly similar to those calculated for the D_{2d} and C_{2v} dimers (Table 6). The rather large ellipticity ( ) value readily confirms the strong interaction of the π electrons.

Table 4 Comparison of the balance between dispersion and exchange repulsion with the number of contacts in ethylene dimers, according to SAPT analysis performed with the aug-cc-pVDZ basis set

Dimer	σ↔σ	σ↔π	π↔π	Total	−EX/DISP
D_{2d}	4	4	1	9	0.95
C_i	0	4	1	5	1.00
C_{2v}	0	2	1	3	1.29

Electrostatic interaction

From the SAPT analysis, all three ethylene dimer conformations show attractive electrostatic interactions—even the D_{2d} dimer with close dihydrogen contacts. This indicates that close contact of the positively charged hydrogen atoms does not necessarily imply electrostatic destabilization overall. The largest stabilizing component is dispersion. However, in the equilibrium geometry, this attractive term has almost the same magnitude as the exchange repulsion, making the net interaction energy close to the electrostatic stabilization contribution. To confirm the roles of dispersion and the electrostatic interaction in the intermolecular binding, several substituted CH···CH ethylene dimers $(RHC{=}CHR)_2$, where $R{=}NH_2$, OH, Cl, F, and CN, have been examined. The structures were optimized with the D_{2d} symmetry constraint (expect for $R{=}NH_2$ and OH, which were optimized with the D_2 and C_2 constraints, respectively). The optimized geometries and results of the SAPT analysis of these substituted dimers are given in Fig. S3 of the ESM and Table 7, respectively. Electron-donating groups (NH_2 and OH) increase the interaction energy, and vice versa for electron-withdrawing groups (Cl, F, and CN). Intriguingly, there is a very strong correlation (R^2=0.99, Fig. S4 in the ESM) between the calculated interaction energy (CCSD(T)/CBS or DFT-SAPT) and the DFT-SAPT electrostatic term. On the other hand, the correlation with the dispersion component is rather poor, R^2=0.20 (see Fig. S4 in the ESM). Hence, we may conclude that dispersion and electrostatic interactions play different roles in dimer

Table 5 Numbers of contacts, SAPT components, and total interaction energies (in kcal mol^{-1}) of ethylene dimers, ethane dimers, and butadiene dimer

Species	Contact	−EX/DISP	ES	EX	DISP	CBS[c]
$(Ethylene)_2$ D_{2d} [a]	9	0.95	−1.21	2.64	−2.43	−1.50
$(Ethylene)_2$ C_i [a]	5	1.00	−1.04	2.07	−1.80	−1.13
$(Ethylene)_2$ C_{2v} [a]	3	1.29	−1.22	2.96	−2.30	−1.08
$(Ethane)_2S_4$ [a]	8	1.03	−1.01	3.10	−3.01	−1.50
$(Ethane)_2$ D_{2d} [a]	4	1.11	−1.00	3.18	−2.88	−1.36
$(Butadiene)_2$ π···π [b]	14	1.14	−3.17	6.88	−6.03	−2.47
$(Butadiene)_2$ CH···π [b]	13	1.18	−2.50	5.85	−4.97	−1.97

[a] SAPT/aug-cc-pVDZ calculation

[b] DFT-SAPT/aug-cc-pVDZ calculation

[c] Interaction energy calculated at the CCSD(T)/CBS level

binding. Dispersion determines the nature of binding and is a more important influence on the interaction distance, while the electrostatic interaction plays an important role in determining the magnitude of the interaction energy at the equilibrium distance. This finding is in agreement with the results from a study on the benzene dimer performed by Hobza and Kim et al. [27].

Interestingly, the D_{2d} dimer shows an electrostatic attraction as large as that of the C_{2v} dimer. What is the origin of this

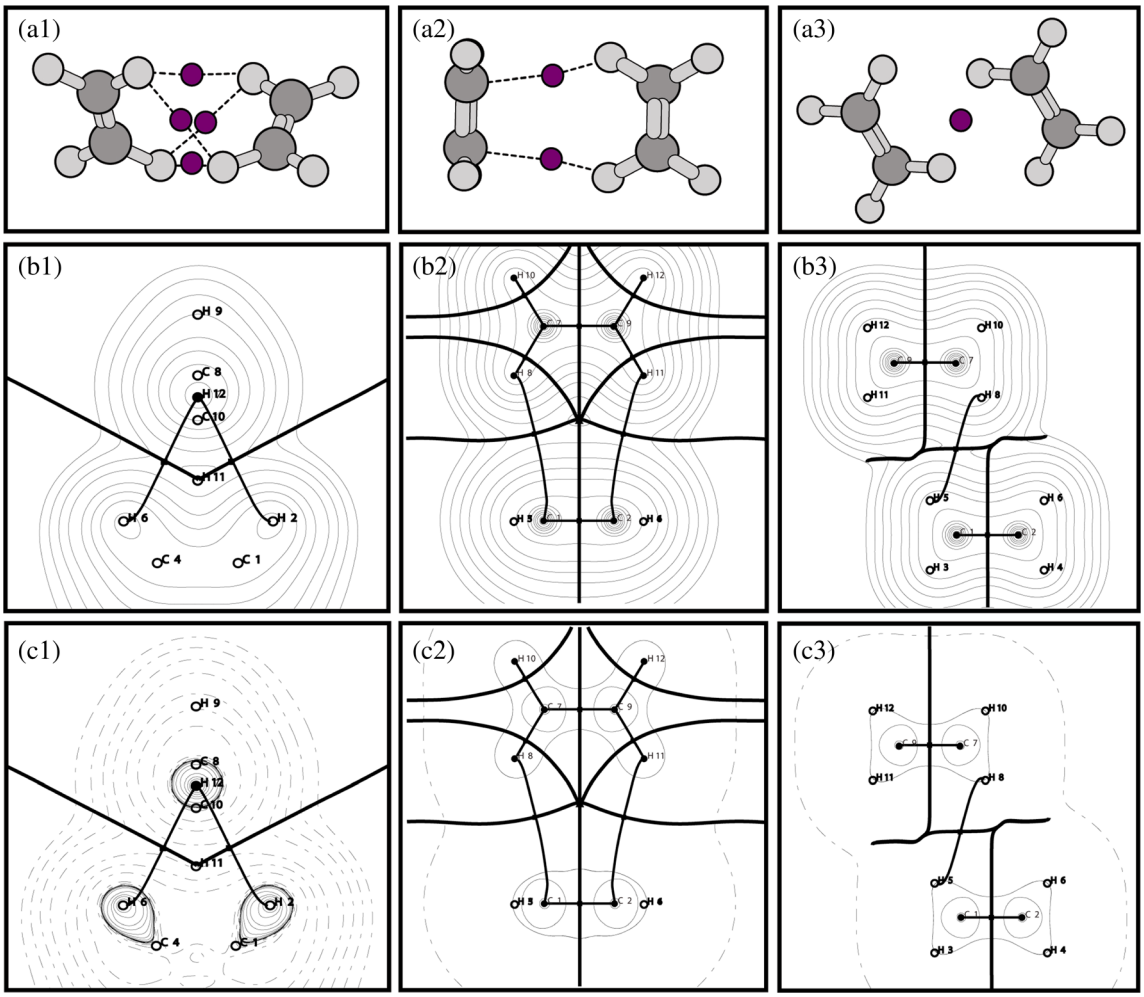

Fig. 6 Plots of **a** bond critical points, **b** electron density contours, and **c** contours of the Laplacian of electron density for the D_{2d}, C_{2v}, and C_i ethylene dimers

Table 6 Calculated topological properties (in atomic units) at bond critical points (BCP), based on AIM analysis using the MP2/aug-cc-pVDZ wavefunction

Property	D_{2d}	C_i	C_{2v}
No. of BCPs	4	1	2
ρ	0.0044	0.0042	0.0055
$\nabla^2\rho$	0.0174	0.0157	0.0166
$\in$	0.8216	78.5804	0.1800

significant attraction? To answer this question, we calculated electrostatic interaction energies using an approach based on the interaction of distributed multipole moments [66, 67] on each monomer. The multipole moments on all atoms are divided into three groups: charges and dipoles (group A), the quadrupole that describes the π-cloud (group C), and the other quadrupoles that describe the charge distribution in the molecular plane (group B). To avoid convergence problems, the dimers were maintained in the same relative orientation, but the intermolecular distance was scaled up to 5 Å. The calculated electrostatic interaction energies among these three groups are listed in Table 8. For the C_{2v} and C_i dimers, the electrostatic attraction is clearly dominated by the quadrupole interaction of the π-cloud, and the interaction is larger for the C_{2v} dimer than for the C_i dimer, which validates the use of the π-atom model for these two structures [17]. For the D_{2d} dimer, the quadrupole interaction between the π-cloud is repulsive. However, the cross-interactions between quadrupoles of different types (those representing the π-cloud and those the molecular plane) increase the attractiveness of the total electrostatic interaction. Since the H atoms are on the outer rim of the ethylene molecular plane, they are the most accessible to intermolecular interactions. The quadrupole moments representing the π-cloud are mostly on C atoms. Therefore, such a cross-quadrupole interaction could be interpreted as a special type of C···H interaction. It appears that the proposed Coulomb interaction model [30] based on bond dipoles is insufficient to describe the electrostatic interaction in the D_{2d} ethylene dimer.

Table 7 DFT-SAPT components and CCSD(T)/CBS interaction energies (in kcal mol^{-1}) of various substituted ethylene dimers [$(RHC{=}CHR)_2$, R=NH_2, OH, H, Cl, F, and CN]

	NH_2	OH	H	Cl	F	CN
r_{CM} (Å)	3.611	3.605	3.707	3.590	3.700	3.726
ES	−2.34	−2.15	−1.25	−0.27	0.27	3.86
EX	4.33	4.04	2.65	3.99	2.10	2.27
IND [a]	−0.13	−0.16	−0.08	−0.38	−0.22	−0.79
DISP	−3.85	−3.38	−2.74	−3.69	−2.28	−2.87
TOT	−2.31	−1.99	−1.59	−0.58	−0.24	2.43
CBS [b]	−2.15	−1.90	−1.50	−0.69	−0.19	2.25

[a] Dispersion is scaled up by 15 %

[b] Interaction energy calculated at the CCSD(T)/CBS level

Table 8 Electrostatic interaction energies (in kcal mol^{-1}) decomposed to multipole interactions for ethylene dimers

Monomer 1	Monomer 2	D_{2d}	C_i	C_{2v}
Group A	Group A	−0.0064	−0.0092	−0.0074
Group A	Group B	0.0062	0.0014	−0.0006
Group A	Group C	0.0182	0.0443	0.0357
Group B	Group A	0.0062	0.0014	−0.0004
Group B	Group B	0.0077	−0.0023	−0.0020
Group B	Group C	−0.0548	−0.0023	0.0075
Group C	Group A	0.0182	0.0443	0.0316
Group C	Group B	−0.0548	−0.0023	0.0361
Group C	Group C	0.0519	−0.2186	−0.2413

Conclusions

This study focused on the nature of the binding of each of the three ethylene dimer configurations D_{2d}, C_i, and C_{2v}. The D_{2d} dimer, which is characterized by four pairs of dihydrogen contacts and the largest dispersion term, is the most stable form. The other two configurations, the C_i and C_{2v} dimers, are almost equal in net interaction energy. Unlike the benzene dimer, the displaced parallel (C_i) dimer is not a stable structure. The stacking effect of π electrons is not significant in this very small π-containing system.

All three ethylene dimers have negative electrostatic interaction energies. Similar to benzene dimers, the largest stabilizing force in ethylene dimers is dispersion. However, this contribution to the stabilization is of almost the same magnitude as the exchange repulsion at the equilibrium distance. As a consequence, the electrostatic interaction is a significant influence on the interaction energies at the equilibrium distances of these ethylene dimers. The electrostatic stabilizations of C_{2v} and C_i dimers are readily described by π atoms. In the case of the D_{2d} dimer, it is important to consider the special attraction between C and H atoms to explain the attractive electrostatic term. As also seen in other neutral π-complexes, induction and induction–dispersion are very small in all three ethylene dimers.

For all three ethylene dimers, dispersion can arise from a π↔π, σ↔π, or σ↔σ (electron pair)–(electron pair) interaction. The σ↔π interaction is favored over the π↔π interaction, even in the displaced parallel dimer, probably because the system is too small. The σ↔σ interaction, which is unique to the D_{2d} dimer, does indeed exist. It helps to stabilize the D_{2d} dimer by increasing the number of electron-pair interactions in dispersion to alter the exchange–dispersion balance. A concept of "contact" was introduced to describe such a balance. A

larger number of contacts will help to reduce intermolecular distance, and in complexes where the attractive electrostatic interaction determines the degree of intermolecular binding strength, this usually means greater stability.

Acknowledgments YC would like to thank the National University of Singapore for the award of a President's Graduate Fellowship.

References

1. Baev AK (2012) Specific intermolecular interactions of organic compounds. Springer, Berlin
2. Hobza P, Müller-Dethlefs K (2010) Non-covalent interactions: theory and experiment. RSC Theoretical and Computational Chemistry Series. Royal Society of Chemistry, London
3. Kaplan IG (2006) Intermolecular interactions: physical picture, computational methods and model potentials. Wiley, Chichester
4. Clark T, Hennemann M, Murray JS, Politzer P (2007) J Mol Model 13:291–296
5. Singh NJ, Min SK, Kim DY, Kim KS (2009) J Chem Theory Comput 5:515–529
6. Podeszwa R, Bukowski R, Szalewicz K (2006) J Phys Chem A 110: 10345–10354
7. Fujii A, Shibasaki K, Kazama T, Itaya R, Mikami N, Tsuzuki S (2008) Phys Chem Chem Phys 10:2836–2843
8. Shibasaki K, Fujii A, Mikami N, Tsuzuki S (2007) J Phys Chem A 111:753–758
9. Tsuzuki S (2005) In: Wales D (ed) Intermolecular forces and clusters I. Structure and Bonding Series, Vol. 115. Springer, Heidelberg, pp. 149–193
10. Soteras I, Orozco M, Luque FJ (2008) Phys Chem Chem Phys 10: 2616–2624
11. Kim D, Tarakeshwar P, Kim KS (2004) J Phys Chem A 108:1250–1258
12. Nishio M (2011) Phys Chem Chem Phys 13:13873–13900
13. Nishio M (2004) CrystEngComm 6:130–156
14. Nishio M, Hirota M, Umezawa Y (1998) The CH–π interaction: evidence, nature, and consequences. Methods in Stereochemical Analysis Series. Wiley, New York
15. Morita SI, Fujii A, Mikami N, Tsuzuki S (2006) J Phys Chem A 110: 10583–10590
16. Tsuzuki S, Honda K, Uchimaru T, Mikami M, Fujii A (2006) J Phys Chem A 110:10163–10168
17. Hunter CA, Sanders JKM (1990) J Am Chem Soc 112:5525–5534
18. Sinnokrot MO, Sherrill CD (2004) J Am Chem Soc 126:7690–7697
19. Sinnokrot MO, Sherrill CD (2004) J Phys Chem A 108:10200–10207
20. Kim KS, Karthikeyan S, Singh NJ (2011) J Chem Theory Comput 7: 3471–3477
21. Sinnokrot MO, Valeev EF, Sherrill CD (2002) J Am Chem Soc 124: 10887–10893
22. Tsuzuki S, Honda K, Uchimaru T, Mikami M, Tanabe K (2002) J Am Chem Soc 124:104–112
23. Pitonak M, Neogrady P, Rezac J, Jurecka P, Urban M, Hobza P (2008) J Chem Theory Comput 4:1829–1834
24. Wang W, Hobza P (2008) ChemPhysChem 9:1003–1009
25. Podeszwa R, Szalewicz K (2008) Phys Chem Chem Phys 10:2735–2746
26. Rube M, Bludsk O, Nachtigall P (2008) ChemPhysChem 9:1702–1708
27. Lee EC, Kim D, Jurecka P, Tarakeshwar P, Hobza P, Kim KS (2007) J Phys Chem A 111:3446–3457
28. Suzuki K, Iguchi K (1982) J Chem Phys 77:4594–4603
29. Alberts IL, Rowlands TW, Handy NC (1988) J Chem Phys 88:3811–3816
30. Tsuzuki S, Tanabe K (1992) J Phys Chem 96:10804–10808
31. King RA (2009) Mol Phys 107:789–795
32. Jurecka P, Sponer J, Cerny J, Hobza P (2006) Phys Chem Chem Phys 8:1985–1993
33. Zhao Y, Truhlar DG (2005) J Phys Chem A 109:5656–5667
34. Matta CF, Hernndez-Trujillo J, Tang T, Bader RFW (2003) Chem Eur J 9:1940–1951
35. Novoa JJ, Whangbo M-H, Williams JM (1991) J Chem Phys 94: 4835–4841
36. Echeverria J, Aullon G, Danovich D, Shaik S, Alvarez S (2011) Nat Chem 4:323–330
37. Grimme S (2008) Angew Chem Int Ed 47:3430–3434
38. Jurecka P, Hobza P (2002) Chem Phys Lett 365:89–94
39. Helgaker T, Klopper W, Koch H, Noga J (1997) Chem Phys 106: 9639–9646
40. Frisch MJ, Trucks GW, Schlegel HB, Scuseria GE, Robb MA, Cheeseman JR, Montgomery JA Jr, Vreven T, Kudin KN, Burant JC, Millam JM, Iyengar SS, Tomasi J, Barone V, Mennucci B, Cossi M, Scalmani G, Rega N, Petersson GA, Nakatsuji H, Hada M, Ehara M, Toyota K, Fukuda R, Hasegawa J, Ishida M, Nakajima T, Honda Y, Kitao O, Nakai H, Klene M, Li X, Knox JE, Hratchian HP, Cross JB, Bakken V, Adamo C, Jaramillo J, Gomperts R, Stratmann RE, Yazyev O, Austin AJ, Cammi R, Pomelli C, Ochterski JW, Ayala PY, Morokuma K, Voth GA, Salvador P, Dannenberg JJ, Zakrzewski VG, Dapprich S, Daniels AD, Strain MC, Farkas O, Malick DK, Rabuck AD, Raghavachari K, Foresman JB, Ortiz JV, Cui Q, Baboul AG, Clifford S, Cioslowski J, Stefanov BB, Liu G, Liashenko A, Piskorz P, Komaromi I, Martin RL, Fox DJ, Keith T, Al-Laham MA, Peng CY, Nanayakkara A, Challacombe M, Gill PMW, Johnson B, Chen W, Wong MW, Gonzalez C, Pople JA (2004) Gaussian 03. Gaussian Inc., Wallingford
41. Jeziorski B, Moszynski R, Szalewicz K (1994) Chem Rev 94:1887–1930
42. Patkowski K, Szalewicz K, Jeziorski B (2006) J Chem Phys 125: 154107–154120
43. Williams HL, Chabalowski CF (2001) J Phys Chem A 105:646–659
44. Hesselmann A, Jansen G, Schutz M (2005) J Chem Phys 122:14103–14107
45. Podeszwa R, Szalewicz K (2005) Chem Phys Lett 412:488–493
46. Werner HJ, Knowles PJ (2008) MOLPRO, version 2008.1, University of Birmingham, Birmingham
47. Polly R, Werner H-J, Manby FR, Knowles PJ (2004) Mol Phys 102: 2311–2321
48. Bukowski R, Cencek W, Jankowski P, Jeziorska M, Jeziorski B, Kucharski SA, Lotrich VF, Misquitta AJ, Moszynski R, Patkowski K, Podeszwa R, Rybak S, Szalewicz K, Williams HL, Wheatley RJ, Wormer PES, Zuchoski PS (2008) SAPT2008: an ab initio program for many-body symmetry-adapted perturbation theory calculations of intermolecular interaction energies. Department of Physics and Astronomy, University of Delaware, Newark
49. Rezac J, Hobza P (2011) J Chem Theory Comput 7:685–689
50. Patkowski K, Szalewicz K (2007) J Chem Phys 127:164103–164117
51. Popelier PLA (1998) MORPHY 98. UMIST, Manchester
52. Stone AJ (2006) Distributed Multipole Analysis of Gaussian Wavefunctions, version 2.2.02. http://www-stone.ch.cam.ac.uk/documentation/gdma/manual.pdf
53. Stone AJ, Dullweber A, Engkvist O, Fraschini E, Hodges MP, Meredith A, Popelier PLA, Wales DJ (2011) ORIENT, version 4.6. University of Cambridge, Cambridge
54. Tsuzuki S, Uchimaru T, Mikami M, Tanabe K (1996) Chem Phys Lett 252:206–210
55. Pittner J, Hobza P (2004) Chem Phys Lett 390:496–499
56. Wormer PES, van der Avoird A (1975) J Chem Phys 62:3326–3339

57. Hobza P, Havlas Z (2000) Chem Rev 100:4253–4264
58. Ran J, Wong MW (2006) J Phys Chem A 110:9702–9709
59. Ringer AL, Figgs MS, Sinnokrot MO, Sherrill CD (2006) J Phys Chem A 110:10822–10828
60. Tekin A, Jansen G (2007) Phys Chem Chem Phys 9:1680–1687
61. Bader R (1994) Atoms in molecules: a quantum theory. Clarendon, Oxford
62. Popelier P (2000) Atoms in molecules: an introduction. Prentice Hall, London
63. Koch U, Popelier PLA (1995) J Phys Chem 99:9747–9754
64. Ran J, Wong MW (2009) Aust J Chem 62:1062–1067
65. Novoa JJ, Mota F (2000) Chem Phys Lett 318:345–354
66. Stone A (1981) Chem Phys Lett 83:233–239
67. Stone A (1997) The theory of intermolecular forces. Clarendon, Oxford